Supplementary information for the article 'Improved branched multi-point approximation method and its application in spacecraft topology optimization'

Abstract

This document serves as a supplement to the research article. In section 1, the concise overview of the construction process for the branched multi-point approximation (BMA) function is provided, highlighting the distinctive characteristics of its functional form. Section 2 provides detailed procedures and results of random numerical experiments conducted on approximation functions. Section 3 presents the interface of the optimization system after secondary development, and outlines some of the Patran command language (PCL) stream utilized in this work and their respective functionalities.

1. Construction of the branched multi-point approximation function

The form of the approximation function is shown in Equation (1). $w^{(p)}(\boldsymbol{Y},\boldsymbol{\alpha})$ is the weighted form of the Taylor expansion function at the *p*-th iteration. Physical quantities such as frequency, mass, and von mises stress are approximated and calculated using $w^{(p)}(\boldsymbol{X},\boldsymbol{\alpha})$. $w(\boldsymbol{X}_t,\boldsymbol{\alpha}_t)$ and $\partial w(\boldsymbol{X}_t,\boldsymbol{\alpha}_t)/\partial x_k$ are the function value and partial derivative value at the known point, respectively. $\tilde{w}$ is the numerical term containing the first derivative information of different variables. $h_t(\boldsymbol{X},\boldsymbol{\alpha})$ is the weighting factor of the *t*-th known point.

$$w^{(p)}(\boldsymbol{X},\boldsymbol{\alpha})=\sum_{t=1}^{H}\left\{w(\boldsymbol{X}_t,\boldsymbol{\alpha}_t)+\sum_{k=1}^{m}\tilde{w}_{k,t}(\boldsymbol{X},\boldsymbol{\alpha})\right\}h_t(\boldsymbol{X},\boldsymbol{\alpha}) \tag{1}$$

where,

$$\tilde{w}_{k,t}(\boldsymbol{X},\boldsymbol{\alpha})=\begin{cases}\dfrac{1}{r_{o,t}}\dfrac{\partial w(\boldsymbol{X}_t,\boldsymbol{\alpha}_t)}{\partial x_k}x_{kt}^{1-r_{o,t}}\left(x_k^{r_{o,t}}-x_{kt}^{r_{o,t}}\right) & \text{if } x_k \text{ and } x_{k,t}\in \boldsymbol{X}_k^{I}\\ \dfrac{1}{r_{m,t}}\dfrac{\partial w(\boldsymbol{X}_t,\boldsymbol{\alpha}_t)}{\partial x_k}\left(1-e^{-r_{m,t}(x_k-x_{kt})}\right) & \text{if } x_k \text{ or } x_{k,t}\in \boldsymbol{X}_k^{II}\end{cases} \tag{2}$$

$$h_t(\boldsymbol{X},\boldsymbol{\alpha})=\frac{\bar{h}_t(\boldsymbol{X},\boldsymbol{\alpha})}{\sum_{l=1}^{H}\bar{h}_l(\boldsymbol{X},\boldsymbol{\alpha})},\quad t=1,\cdots,H \tag{3}$$

$$\bar{h}_l(\boldsymbol{X},\boldsymbol{\alpha})=\prod_{\substack{s=1\\ s\neq l}}^{H}(\boldsymbol{X}-\boldsymbol{X}_s)^{\mathrm{T}}(\boldsymbol{X}-\boldsymbol{X}_s) \tag{4}$$

The following provides a brief explanation of the characteristics of branched multi-point approximation (BMA) function in its construction.

✧ The characteristics of weighting function $h_t(\boldsymbol{X},\boldsymbol{\alpha})$. $h_t(\boldsymbol{X},\boldsymbol{\alpha})$ satisfies the following relationship:

Supplement

$$\begin{cases} 0 \le h_t(\boldsymbol{X},\boldsymbol{\alpha}) \le 1 \\ \sum_{t=1}^{H} h_t(\boldsymbol{X},\boldsymbol{\alpha}) = 1.0 \end{cases} \tag{5}$$

Essentially, $h_t(\boldsymbol{X},\boldsymbol{\alpha})$ is an interpolation function, the form of which ensures that the function values and gradients of the approximation function are indeed accurate at the known points.

✧ When employing the power function $\varphi(\boldsymbol{X}) = x_k^{r_{o,t}}$ as an intermediate variable, the first-order Taylor expansion of $w(\boldsymbol{X},\boldsymbol{\alpha})$ at point $(\boldsymbol{X}_t,\boldsymbol{\alpha}_t)$ is derived as follows.

$$\begin{aligned} w^{(p)}(\boldsymbol{X},\boldsymbol{\alpha}) &= w(\boldsymbol{X}_t,\boldsymbol{\alpha}_t) + \sum_{k=1}^{m} \frac{\partial w(\boldsymbol{X}_t,\boldsymbol{\alpha}_t)}{\partial \varphi(\boldsymbol{X})} (\varphi(\boldsymbol{X}) - \varphi(\boldsymbol{X}_t)) \\ &= w(\boldsymbol{X}_t,\boldsymbol{\alpha}_t) + \sum_{k=1}^{m} \frac{\partial w(\boldsymbol{X}_t,\boldsymbol{\alpha}_t)}{\partial x_k} \cdot \frac{\partial x_k}{\partial \varphi(\boldsymbol{X})} (x_k^{r_{o,t}} - x_{kt}^{r_{o,t}}) \end{aligned} \tag{6}$$

Since $\frac{\partial \varphi(\boldsymbol{X})}{\partial x_k} = \frac{\partial (x_k^{r_{o,t}})}{\partial x_k} = r_{o,t} \cdot x_k^{r_{o,t}-1}$, we update $w^{(p)}(\boldsymbol{X},\boldsymbol{\alpha})$ as follows.

$$w^{(p)}(\boldsymbol{X},\boldsymbol{\alpha}) = w(\boldsymbol{X}_t,\boldsymbol{\alpha}_t) + \sum_{k=1}^{m} \frac{1}{r_{o,t}} \frac{\partial w(\boldsymbol{X}_t,\boldsymbol{\alpha}_t)}{\partial x_k} y_{kt}^{1-r_{o,t}} (x_k^{r_{o,t}} - x_{kt}^{r_{o,t}}) \tag{7}$$

✧ When employing the exponential function $\varphi(\boldsymbol{X}) = e^{-r_{m,t}x_k}$ as an intermediate variable, the first-order Taylor expansion of $w(\boldsymbol{X},\boldsymbol{\alpha})$ at point $(\boldsymbol{X}_t,\boldsymbol{\alpha}_t)$ is derived as follows.

$$\begin{aligned} w^{(p)}(\boldsymbol{X},\boldsymbol{\alpha}) &= w(\boldsymbol{X}_t,\boldsymbol{\alpha}_t) + \sum_{k=1}^{m} \frac{\partial w(\boldsymbol{X}_t,\boldsymbol{\alpha}_t)}{\partial \varphi(\boldsymbol{X})} (\varphi(\boldsymbol{X}) - \varphi(\boldsymbol{X}_t)) \\ &= w(\boldsymbol{X}_t,\boldsymbol{\alpha}_t) + \sum_{k=1}^{m} \frac{\partial w(\boldsymbol{X}_t,\boldsymbol{\alpha}_t)}{\partial x_k} \cdot \frac{\partial x_k}{\partial \varphi_k(\boldsymbol{X})} (e^{-r_{m,t}x_k} - e^{-r_{m,t}x_{kt}}) \end{aligned} \tag{8}$$

Since $\frac{\partial \varphi(\boldsymbol{X})}{\partial x_k} = \frac{\partial (e^{-r_{m,t}x_k})}{\partial x_k} = -r_{m,t} e^{-r_{m,t}x_k}$, we update $w^{(p)}(\boldsymbol{X},\boldsymbol{\alpha})$ as follows.

$$w^{(p)}(\boldsymbol{X},\boldsymbol{\alpha}) = w(\boldsymbol{X}_t,\boldsymbol{\alpha}_t) + \sum_{k=1}^{m} \frac{1}{r_{m,t}} \frac{\partial w(\boldsymbol{X}_t,\boldsymbol{\alpha}_t)}{\partial x_k} (1 - e^{-r_{m,t}(x_k - x_{kt})}) \tag{9}$$

For each continuous variable x_k, Equation (2) determines whether to employ Equation (7) or Equation (9) to construct the approximation function, contingent upon the known points and the current topological form of the individual. The power function form of approximation is utilized only when both A and B belong to C. Otherwise, an exponential function form of approximation is employed. Due to the smoother nature of power functions, they are preferred for cross-domain approximations.

Here, a combination of power functions and exponential functions is employed to construct the approximation function, balancing the computational efficiency and the stability of the approximation. The discrete variable $\boldsymbol{\alpha}$ only affects the segmentation of the function.

2. Randomized numerical simulation of approximation function

Supplement

This section explores the approximation ability of different approximation methods in discontinuous domains, and compares the approximation scheme of this work with four other potential schemes. In reality, methods to study the approximation effects of 'approximate functions with discrete variables' are scarce. This section introduces a randomized simulation approach to examining the approximation performance of such functions.

2.1 Five approximate schemes

Listed below are five potential different approximation schemes for $\tilde{w}_{k,t}(\boldsymbol{X},\boldsymbol{\alpha})$ in Equation (1), for ease of reference in section 2.2 and 2.3.

Approximation method 1: The segmentation of approximate function is determined solely based on the topological form of the known point $\boldsymbol{\alpha}_t$. Concisely, if the continuous variable associated with the known point adheres to $x_{kt} \in \boldsymbol{X}_k^I$, a power function $y_k = x_k^r$ serves as an intermediary to carry out a weighted approximation in the form of Taylor series. Otherwise, an exponential function $y_k = e^{-rx_k}$ is employed. In mathematical terms,

$$\tilde{w}_{k,t}(\boldsymbol{X},\boldsymbol{\alpha}) = \begin{cases} \dfrac{1}{r_{o,t}} \dfrac{\partial w(\boldsymbol{X}_t,\boldsymbol{\alpha}_t)}{\partial x_k} x_{kt}^{1-r_{o,t}} (x_k^{r_{o,t}} - x_{kt}^{r_{o,t}}) & \text{if} \quad x_{kt} \in \boldsymbol{X}_k^I \\ \dfrac{1}{r_{m,t}} \dfrac{\partial w(\boldsymbol{X}_t,\boldsymbol{\alpha}_t)}{\partial x_k} (1 - e^{-r_{m,t}(x_k - x_{kt})}) & \text{if} \quad x_{kt} \in \boldsymbol{X}_k^{II} \end{cases} \tag{10}$$

Approximation method 2: As in Ref[1], the segmentation of function is determined solely based on the topological form of the current point $\boldsymbol{\alpha}$. In mathematical terms,

$$\tilde{w}_{k,t}(\boldsymbol{X},\boldsymbol{\alpha}) = \begin{cases} \dfrac{1}{r_{o,t}} \dfrac{\partial w(\boldsymbol{X}_t,\boldsymbol{\alpha}_t)}{\partial x_k} x_{kt}^{1-r_{o,t}} (x_k^{r_{o,t}} - x_{kt}^{r_{o,t}}) & \text{if} \quad x_k \in \boldsymbol{X}_k^I \\ \dfrac{1}{r_{m,t}} \dfrac{\partial w(\boldsymbol{X}_t,\boldsymbol{\alpha}_t)}{\partial x_k} (1 - e^{-r_{m,t}(x_k - x_{kt})}) & \text{if} \quad x_k \in \boldsymbol{X}_k^{II} \end{cases} \tag{11}$$

Approximation method 3: Please refer to Equation (2). The segmentation of function is determined based on the disparity between the topological form of the current point $\boldsymbol{\alpha}$ and known point $\boldsymbol{\alpha}_t$, rather than being solely reliant on one of them.

Approximation method 4: Only intermediate variables in the form of power function $y_k = x_k^r$ are utilized for weighted approximation. In mathematical terms,

$$\tilde{w}_{k,t}(\boldsymbol{X},\boldsymbol{\alpha}) = \frac{1}{r_{o,t}} \frac{\partial w(\boldsymbol{X}_t,\boldsymbol{\alpha}_t)}{\partial x_k} x_{kt}^{1-r_{o,t}} (x_k^{r_{o,t}} - x_{kt}^{r_{o,t}}) \tag{12}$$

Approximation method 5: Only intermediate variables in the form of exponential function $y_k = e^{-rx_k}$ are utilized for weighted approximation. In mathematical terms,

$$\tilde{w}_{k,t}(\boldsymbol{X},\boldsymbol{\alpha}) = \frac{1}{r_{m,t}} \frac{\partial w(\boldsymbol{X}_t,\boldsymbol{\alpha}_t)}{\partial x_k} (1 - e^{-r_{m,t}(x_k - x_{kt})}) \tag{13}$$

The average error function, $\overline{REMS}$, is established to assess the accuracy of different approximation methods.

$$\overline{REMS} = \frac{1}{Q} \sum_{j=1}^{Q} REMS_j = \frac{1}{Q} \sum_{j=1}^{Q} \sqrt{\sum_{(\boldsymbol{X},\boldsymbol{\alpha}) \subseteq \Omega} \left(w^{(\cdot)}(\boldsymbol{X},\boldsymbol{\alpha}) - w(\boldsymbol{X},\boldsymbol{\alpha}) \right)^2} \tag{14}$$

where, $w^{(\cdot)}(\boldsymbol{X},\boldsymbol{\alpha})$ represents the predicted value of the response at point $(\boldsymbol{X},\boldsymbol{\alpha})$ by the multi-point approximation function, i.e. Equation (1); $w(\boldsymbol{X},\boldsymbol{\alpha})$ denotes the actual response value; Q signifies the total number of tests conducted with Q=20000. In each test, the sample points (i.e., known points) are randomly selected according to a predetermined topological configuration. $REMS_j$ represents the approximation error of the function constructed using these

Supplement

points in *j*-th test. Ω is the test set, encompassing areas in the vicinty of sample points as well as test points situated between discontinuous domains, as demonstrated in the tabulated data presented in Table 1~Table 4. The term 'vicinity' refers to the area within the range of move limit centered around the known points. Notably, when the approximation function predicts the domain $\boldsymbol{X}_k^{II}$, the test set contains only a single point from that domain. In the following, S^2 denotes the variance of $REMS_j$ after Q tests.

2.2 Numerical analysis of single discrete and single continuous variable

The numerical analysis in this section deals with a single discrete variable, which is uniquely mapped onto a continuous variable. We can establish the approximate function for the mechanical response, using different approximation methods in section 2.1 and sensitivity analysis. The plate model in Fig.1 has the thickness of 2.0 mm, dimensions of 100.0 mm in height and width, and fixed displacement boundaries at its four corners. The plate and beam are made of stainless steel, with material properties such as the elastic modulus of 200GPa, the density of 7800kg/m^3, and the Poisson's ratio of 0.3. The stiffened beam has a circular cross-section with an initial radius of 3.0mm modeled using beam elements in Patran. The discrete variable α_1 indicates if the stiffened beam is present or absent, while the continuous variable x_1 represents the radius of the beam section, with $2.0 \le x_1 \le 4.0$mm when $a_1 = 1$. Based on the weak element technique, when the beam does not exist (i.e., $a_1 = 0$), $x_1^b = 0.01x_1^L$ is taken synchronously.

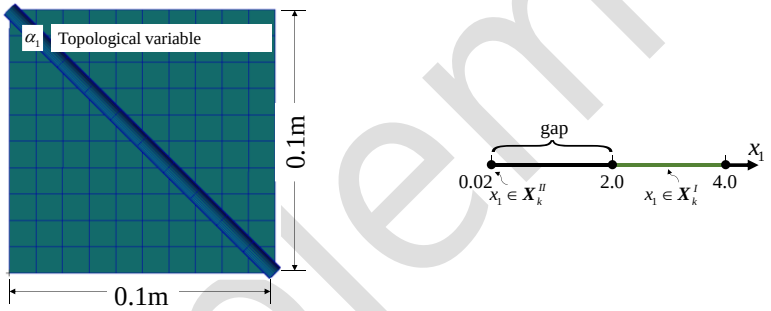

(a)FE model (b)The region division

Fig.1 FE model and design variables' space considering only one discrete variable

Initially, four points with topological forms 0, 1, 1, 1 are randomly picked to analyze the performance of various approximation methods. The results of random test results are presented in Table 1, and the fit quality is visualized in Fig.2(a). If the current point has a topological form $\alpha_1 = 0$, predictions from various approximation functions are precise due to the presence of the known points with topological form 0. Notably, when $\alpha_1 = 1$, the proposed method 3 yields smaller average prediction error and variance. Secondly, four points with topological forms 1, 1, 1, 1 are randomly chosen. The test results are presented in Table 2, and the fit quality is visualized in Fig.2(b). When $\alpha_1 = 1$, the first four methods have the same approximation. If $\alpha_1 = 0$, method 2 aligns with method 3, while method 1 aligns with method 4. Methods 2, 3, and 5 exhibit good approximation in region $\boldsymbol{X}_k^{II}$, known as smoothing between discontinuities. The power function exhibits the characteristic of 'passivation'.

Supplement

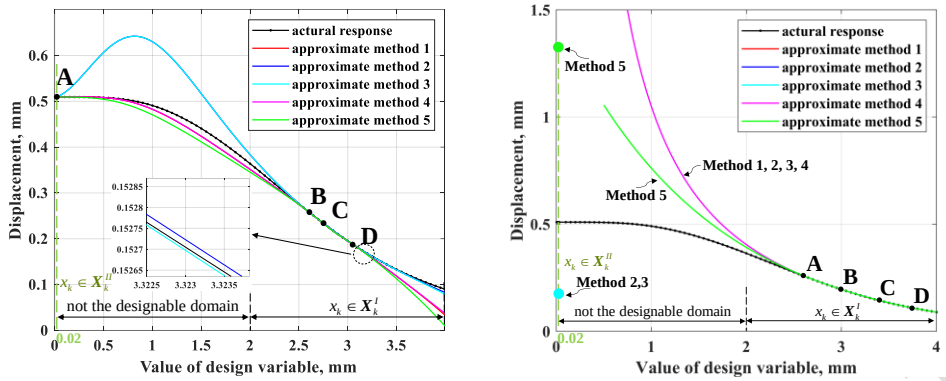

(a) Topological forms of known points are 0, 1, 1, 1 (b) Topological forms of known points are 1, 1, 1, 1

Fig.2 The performance of various approximation methods under a specific test

Table 1. The statistics of approximation effect when known points have topological forms of 0, 1, 1, 1

Method number	Basis of function segmentation	Prediction in the vicinty of point B, C and D (i.e., $\alpha_1 = 1$)*		Prediction in the vicinty of point A (i.e., $\alpha_1 = 0$)**	
		$\overline{REMS}$	S^2	$\overline{REMS}$	S^2
1	Based on known points	0.0402	9.688×10^{-5}	0	0
2	Based on current point	0.0154	3.173×10^{-5}	0	0
3	Based on the disparity	0.0151	2.987×10^{-5}	0	0
4	Only power function is used	0.0408	1.023×10^{-4}	0	0
5	Only exponential function is used	0.0464	1.976×10^{-4}	0	0

Note: *Test set Ω includes all data points after discretizing the vicinity of each point, as is also the case in Table 2. **Test set Ω contains only one data point. That is, taking the continuous variable as the small value.

Table 2. The statistics of approximation effect when known points have topological forms of 1, 1, 1, 1

Method number	Basis of function segmentation	Prediction in the vicinty of all known point (i.e., $\alpha_1 = 1$)		Prediction for $\boldsymbol{X}_k^{II}$ (i.e., $\alpha_1 = 0$)	
		$\overline{REMS}$	S^2	$\overline{REMS}$	S^2
1	Based on known points	0.0058	1.077×10^{-5}	164.57	2.303×10^{5}
2	Based on current point	0.0058	1.077×10^{-5}	0.169	0.0012
3	Based on the disparity	0.0058	1.077×10^{-5}	0.169	0.0012
4	Only power function is used	0.0058	1.077×10^{-5}	164.57	2.303×10^{5}
5	Only exponential function is used	0.0039	4.222×10^{-6}	0.904	0.0447

2.3 Numerical analysis of two discrete and two continuous variables

The numerical analysis in this section deals with two discrete variables, each of which is mapped onto only one continuous variable. The FE model in Fig.3(a) demonstrates the regions governed by each discrete variable (exhibiting variable link). The plate thickness is 2.0mm, and both the height and width of the plate are 100.0mm, with the displacement boundary conditions set as fixed supports at the four corner points. Fig.3(b) describes the feasible region, the infeasible region, and the gap between the two regions. The material parameters, the upper and lower limits of the variables and the cross-section of beam are the same as those of section 2.2, and the initial radius of the stiffened beam is 3.0mm. The weak element technique is also employed.

Supplement

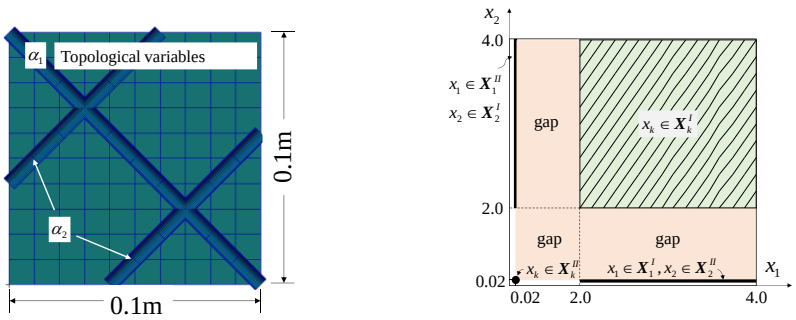

(a)FE model (b)The region division

Fig.3 FE model and design variables' space considering two discrete variables

Initially, four points with topological forms 11, 11, 11and 11 are randomly picked to analyze the performance of various approximation methods. The results of random test are presented in Table 3, and the fit quality is visualized in Fig.4(a). Secondly, four points with topological forms 01, 01, 10 and 10 are randomly chosen. The test results are presented in Table 4, and the fit quality is visualized in Fig.4(b). Both two-dimensional and one-dimensional variable analyses can yield comparable conclusions. That is, relying solely on power functions for approximation in discontinuous domains may introduce significant numerical inaccuracies. Method 1 (based on known points) also exhibits such approximation instability. Although method 5 (only exponential function) is stable across different approximation scenarios, its accuracy is not the highest. And method 3 (based on the disparity) presented in this study has either the same or lower prediction error compared to method 2 (based on current point). Considering both the approximation stability and accuracy, method 3 is the superior approach.

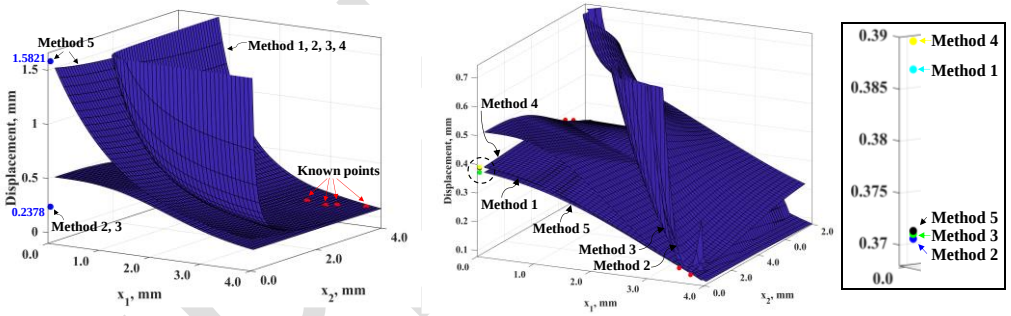

(a) when known points are 11, 11, 11and 11 (b) when known points are 01, 01,10 and 10

Fig.4 The performance of various approximation methods under a specific test

Table 3. The statistics of approximation effect (known points have topological forms of 11, 11, 11, 11)

Method number	Basis of function segmentation	Predictions in the vicinity of all known points		Prediction for $\boldsymbol{\alpha}=01^{*}$		Prediction for $\boldsymbol{\alpha}=00^{**}$	
		$\overline{REMS}$	S^2	$\overline{REMS}$	S^2	$\overline{REMS}$	S^2
1	Based on known points	8.83×10^{-4}	1.40×10^{-7}	3.83×10^{3}	1.98×10^{8}	690.64	5.96×10^{6}
2	Based on current point	8.83×10^{-4}	1.40×10^{-7}	0.6881	0.0233	0.2597	9.52×10^{-4}
3	Based on the disparity	8.83×10^{-4}	1.40×10^{-7}	0.6881	0.0233	0.2597	9.52×10^{-4}
4	Only power function	8.83×10^{-4}	1.40×10^{-7}	3.83×10^{3}	1.98×10^{8}	690.64	5.96×10^{6}
5	Only exponential function	8.31×10^{-4}	1.18×10^{-7}	4.5651	3.0680	0.6887	0.0841

Note: *Test set Ω contains only one data. Point '01': starting from a random known point '11', take the first discrete variable's corresponding continuous variable as the small value, while keeping the second discrete variable's corresponding continuous variable unchanged. **Point '00': two continuous variables are set to the small values, as is also the case in Table 4.

Submitted

Table 4. The statistics of approximation effect (known points have topological forms of 01, 01, 10, 10)

Method number	Basis of function segmentation	Predictions in the vicinity of all known points		Prediction for $\alpha = 11^*$		Prediction for $\alpha = 00$	
		$\overline{REMS}$	S^2	$\overline{REMS}$	S^2	$\overline{REMS}$	S^2
1	Based on known points	0.0042	5.05×10^{-7}	0.269	0.004	0.1144	2.11×10^{-4}
2	Based on current point	0.0013	6.82×10^{-7}	0.421	0.005	0.1314	1.57×10^{-4}
3	Based on the disparity	0.0011	6.92×10^{-7}	0.322	0.004	0.1308	1.52×10^{-4}
4	Only power function	0.0043	5.41×10^{-7}	0.025	2.11×10^{-4}	0.1120	2.16×10^{-4}
5	Only exponential function	0.0097	8.55×10^{-6}	0.271	0.0036	0.1297	1.66×10^{-4}

Note: *Test set Ω contains only one data. Point '11': starting from a random known point '01' or '10', set the continuous variable corresponding to the discrete variable of 0 to its lower limit, while keeping the continuous variable corresponding to the discrete variable of 1 unchanged.

3.The interface of the optimization system

Fig. 5 illustrates the topology optimization interface integrated within Patran, which includes a newly added module named 'Topology_opt'. This optimization interface facilitates the input of optimization parameters, the plotting of iteration curves, and the display of the optimal topological configuration. Upon clicking the 'optimize' button, the topology optimization process is automatically initiated, proceeding to generate and read files, invoke the optimizer, and continue until convergence is achieved or the maximum number of iterations is reached.

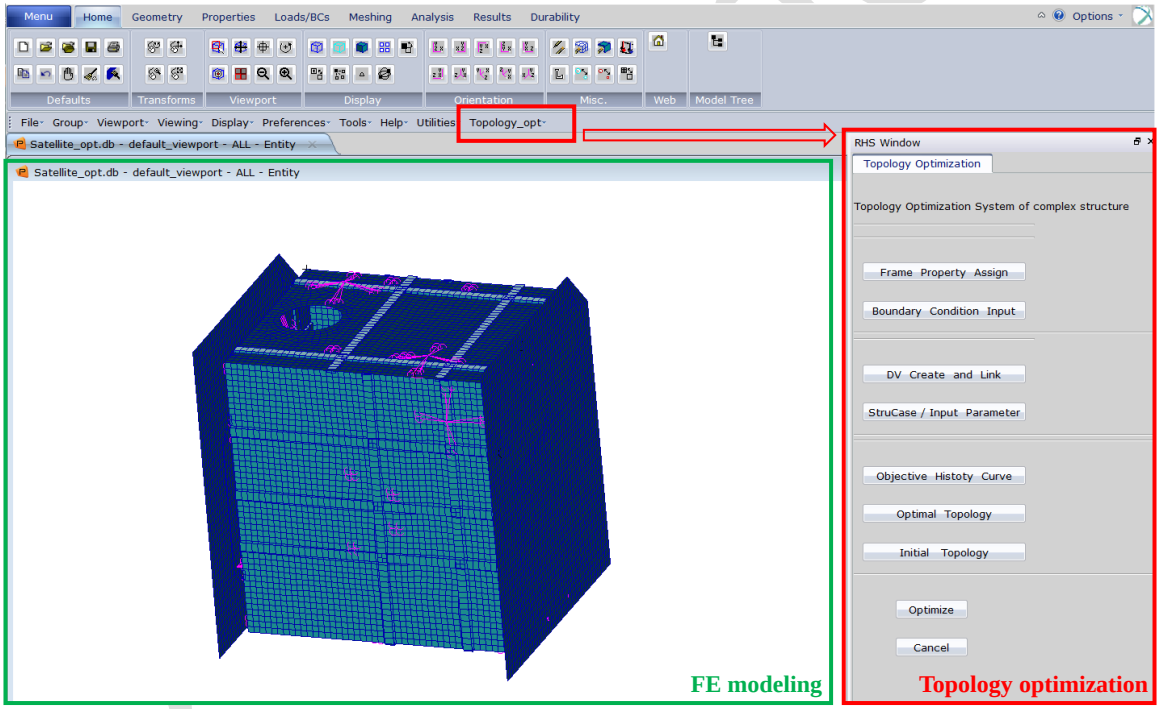

Fig. 5 The interface of the optimization system

The following section outlines some of the Patran command language (PCL) stream utilized in this study, along with their respective meanings. For detailed information regarding the input-output relationships, readers are directed to the reference documentation provided by MSC.Software [2].

- **ui_item_create (parent, name, label, toggleable, options)**

Description: Creates an item widget to be used as a child of a menu, menubar, option menu, or switch widget.

- **ui_label_create (parent, callback, x, y, label)**

Description: Create a label widget. Labels are used only to label other widgets and cannot be selected. They provide additional information to the user.

- **ui_button_create (parent, callback, x, y, width, height, label, [ ], highlight)**

Description: Create a button widget. A button has only one option: it is clicked to initiate an action. No manipulation of data occurs in terms of direct input.

- **ui_separator_create (parent, name, x, y, length, horizontal)**

Description: Create a separator widget.

- **ui_exec_function (class name, function name)**

Description: Invokes a class's function.

- **ui_write (expression, ...)**

Description: Write out a set of expressions, one per line, to the history window.

- **analysis_main.get_job_name_and_desc** (job_name, job_description)

Description: The name of the currently selected job. The maximum length of this string is 31 characters.

- **text_read_string (chan, line, lenline)**

Description: Read a single record into a string from a text I/O file.

- **text_get_position (chan, position)**

Description: Get the current position in the text file for later use with text_set_position.

- **db_count_elements_in_region (region_id, num_elems)**

Description: Get the number of elements associated with the element property region specified by region_id.

- **utl_process_spawn (command, wait)**

Description: The program will execute a “fork” system call (or “vfork”, depending on the specific machine implementation) followed by an “execvp” system call with the “command” specified by the caller as its argument.

The optimizer has been compiled into an executable (.exe) file for ease of invocation. Herein, only a part of the commands is given as an example to illustrate the basis of secondary development.

Reference

[1] Huang H, An HC, et al. An engineering method for complex structural optimization involving both size and topology design variables. International Journal for Numerical Methods in Engineering 2018, 117(3): 291-315.

[2] MSC.Software Corporation. MSC.Nastran Release Guide. Newport Beach: MSC Software Corporation 2018.

Supplement